

## EARLY AGE BEHAVIOUR OF CONCRETE NUCLEAR CONTAINMENTS

Farid Benboudjema<sup>1)</sup> and Jean-Michel Torrenti<sup>1) & 2)</sup>

1) Laboratoire de Mécanique et Technologie, ENS de Cachan, Cachan, France

2) Laboratoire Central des Ponts et Chaussées, Paris, France

### ABSTRACT

Taking into account creep at early-age is essential if one wants to predict quantitatively the induced stresses in concrete structures at early age. Indeed, creep strains may relax internal stresses. In this approach, we use a basic creep model which has been developed previously for aged concrete. This model is then extended to include the effects of hydration, which influences significantly the amplitude of early-age creep. Numerical simulations are performed in order to predict the behaviour of a massive wall. They show that significant relaxation of stresses occur only after about ten days, after cracking occurs. Furthermore, a 3D simulation is necessary in order to be more predictive.

### INTRODUCTION

Concrete containments of nuclear power plants are very massive structures. During the construction, concrete lifts are about three meters high, and the duration between lifts is about 15 days. Two important phenomena are likely to occur.

In the one hand, because the thickness of concrete is equal to 1.2 m, and due to the release of heat during the hydration reaction, a temperature gradient is generated inside the wall, which will induce differential evolutions of hydration degree, thermal strains and autogeneous strains. As soon as the material does not exhibit a sufficient stiffness, induced stresses are very small (compared to the strengths). However, as soon as the stiffness becomes sufficient, there is a risk of crack occurrence.

In the other hand, the cast concrete during the next lift exhibits thermal and autogeneous strains, while the strains of the previously cast concrete are no more significant. Furthermore, the Young modulus of each concrete layer is different. Therefore, the strains in youngest concrete layer are restrained (by the oldest concrete layer) and tensile stresses arise in this element. There is again a risk of crack occurrence through the containment, which can thus promote the leakage of radioactive elements in the environment in the case of an accident, during the service life of the containments.

The prediction of cracking needs a numerical resolution due to the complexity of the young age behaviour of concrete. The following phenomena must be taken into account:

- The evolution of hydration: this is achieved by the use of chemical affinity [1];
- The evolution of temperature: the energy balance equation, which includes the release of heat due to the hydration reaction is solved;
- The evolutions of thermal strains and autogeneous shrinkage;
- The evolution of Young modulus and tensile strength with respect to the hydration degree [2];
- The description of cracking in tension [3];
- Basic creep strains, which will relax induced stresses;
- Drying shrinkage and drying creep: these features are not taken into account since we focus only on massive structures.

In this paper, a model, which takes into account these phenomena, is presented. It has been implemented in a finite elements code (Cast3m, developed by the French Atomic Energy Commission). Numerical simulations are performed and compared to experimental ones obtained by EDF (French Group of electricity) [4,5] on a massive wall (cast with an ordinary concrete).

### CONSTITUTIVE MODEL

#### Chemo-Thermal Model

The hydration of cement paste is a thermo-activated process. Its evolution is modelled by [1]:

$$\dot{x} = \tilde{A}(x) \exp\left(-\frac{E_a}{RT}\right) \quad (1)$$

in which  $\dot{x}$  is the rate of degree of hydration,  $\tilde{A}(x)$  is the normalized affinity,  $E_a$  is the activation energy,  $R$  is the constant of perfect gas and  $T$  is the temperature in Kelvin. The normalized affinity is associated the micro-diffusion process of water which react with unhydrated cement [1].

The evolution of temperature is obtained from the energy balance equation, which includes the release of heat due to the hydration reaction:

$$C \dot{T} = \nabla(k \nabla T) + L \dot{x} \quad (2)$$

in which  $L$  is the latent heat of hydration,  $k$  is the thermal conductivity and  $C$  in volumetric heat capacity, which are kept constant.

### Thermal and autogeneous shrinkage model

The thermal strain  $\epsilon_{th}$  is related to the temperature variation, due to the release of heat by the hydration, and to the thermal dilation coefficient  $\alpha$ . This coefficient is taken constant (in fact it is varying but very soon becomes constant [11]). Autogeneous shrinkage  $\epsilon_{au}$  is related to variation of hydration degree by a constant parameter  $b$ :

$$\epsilon_{th} = \alpha \Delta T \quad \text{and} \quad \epsilon_{au} = -b \Delta x \quad (3)$$

### Elastic-Damage Model

The mechanical behaviour of concrete is modelled by an elastic-damage model coupled with creep, which includes the evolution of the elastic stiffness with respect to the hydration degree (taking from [2]) and with respect to damage [3]. The relationship between apparent stresses  $\sigma$ , effective stresses  $\tilde{\sigma}$ , damage  $D$ , elastic stiffness tensor  $\mathbf{E}$ , elastic strains  $\epsilon_{el}$ , basic creep strains  $\epsilon_{bc}$ , total strains  $\epsilon$ , and previously defined strains reads:

$$\sigma = (1 - D)\tilde{\sigma} \quad \text{and} \quad \tilde{\sigma} = \mathbf{E}(x)\epsilon_{el} = \mathbf{E}(x)(\epsilon - \epsilon_{bc} - \epsilon_{au} - \epsilon_{th}) \quad (4)$$

The Poisson ratio is assumed to be constant and the Young modulus  $E$  increases due to hydration [2]:

$$E(x) = E_{\infty} \bar{x}^b \quad \text{with} \quad \bar{x} = \left\langle \frac{x - x_0}{x_{\infty} - x_0} \right\rangle_+ \quad (5)$$

in which  $x_0$  is the mechanical percolation threshold. It corresponds to the hydration degree below the concrete has negligible mechanical properties (Young modulus, strength ...). It is kept constant and equal to 0.1, which corresponds to the usual value reported by [6].  $x_{\infty}$  is the final hydration degree and  $E_{\infty}$  is the final Young modulus (i.e. when  $x = x_{\infty}$ ) and  $b$  is a constant equal to 0.62 according to [2].  $\langle \cdot \rangle_+$  is to the positive part operator.

$D$  is linked to the elastic equivalent tensile strain  $\hat{\epsilon}$ :

$$\hat{\epsilon} = \sqrt{\langle e_{el} \rangle_+ : \langle e_{el} \rangle_+} \quad (6)$$

$k_0(\xi)$  is the tensile strain threshold. Then,  $D = 0$  if  $\hat{\epsilon} \leq k_0(x)$  and:

$$D = 1 - \frac{k_0}{\hat{\epsilon}} \left[ (1 + A_t) \exp(-B_t \hat{\epsilon}) - A_t \exp(-2B_t \hat{\epsilon}) \right] \quad \text{if} \quad \hat{\epsilon} \geq k_0(\xi) \quad (7)$$

where  $A_t$  and  $B_t$  are constant material parameters which controls the softening branch in the stress-strain curve in tension.

In our application we consider only damage due to tension. The tensile strength evolution reads [2]:

$$f_t(x) = f_{t\infty} \bar{x}^g \quad (8)$$

where  $f_{t\infty}$  is the final tensile strength (i.e. when  $x = x_{\infty}$ ). For a CEM I 52.5, De Schutter and Taerwe [6] found that  $g = 0.46$  fits well experimental data.

The evolution of the tensile strain threshold is then computed from the evolution of tensile strength (Eq. 8) and the Young modulus (Eq. 5):

$$k_0(x) = \frac{f_t(x)}{E(x)} = \frac{f_{t\infty}}{E_{\infty}} \bar{x}^{g-b} \quad (9)$$

Strain softening induces inherent mesh dependency and produces failure without energy dissipation [7]. In order to avoid such shortcomings, a characteristic length  $l_c$  is introduced. This length is related to the mesh size [8,9] in order to dissipate the same amount of energy after mesh refinement, when strains localize in one row of finite elements.

### Basic Creep Model

Many mechanisms for basic creep of concrete have been proposed in order to retrieve all the collected experimental evidences. Even no mechanism has been universally accepted yet, several models exist in the literature.

Several models for basic creep are based on rheological elements (spring and dashpots). The most used elements are Kelvin-Voigt and Maxwell chains, which are combined in serial or/and parallel. Here, we used several Kelvin-Voigt chains (see Figure 1). Hauggaard et al. [10] and de Schutter [2] used only one Kelvin-Voigt unit for the modelling of early-age basic creep.

Hauggaard et al. [10] expresses material parameters as functions of time. The effect of age on basic creep of concrete is, here, taken into account by relating the material parameters to the degree of hydration, since it is more physical. The relationships proposed by de Schutter [2] are slightly modified for the Kelvin-Voigt units: the retardation times  $t_{bc}^i$  (ratios between the stiffness and the associated viscosity) are kept constant. The material parameters read:

$$k_{bc}^i(x) = k_{bc-\infty}^i \frac{0.473}{2.081 - 1.608x} = x^{-0.62} \quad \& \quad t_{bc}^i = \frac{h_{bc}^i(x)}{k_{bc}^i(x)} \quad (10)$$

where  $k_{bc-\infty}^i$  is the final stiffness (i.e. when  $x = x_\infty$ ) of the spring in the Kelvin-Voigt unit  $i$ .

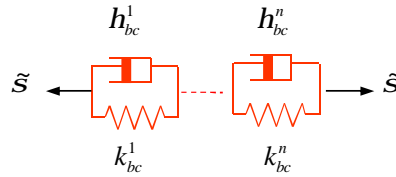


Figure 1. Kelvin-Voigt elements for the prediction of creep strains.

We obtain a non-linear second order differential equation:

$$t_{bc}^i \frac{\partial^2 \tilde{s}}{\partial t^2} + \left( t_{bc}^i \frac{\partial k_{bc}^i(x)}{\partial t} + 1 \right) \frac{\partial \tilde{s}}{\partial t} = \frac{\tilde{s}}{k_{bc}^i(x)} \quad (11)$$

## NUMERICAL SIMULATION OF A CONTAINMENT

### Experiment

During the construction of the Civaux nuclear power plant, a reinforced concrete wall (with prestressing cable ducts) was built in order to evaluate the risk of cracking of the real containment at early age, using two different concrete mixes: an ordinary concrete (OC) and a high performance concrete (HPC). The wall was 1.2 m wide, 1.9 m high, 20 m long and was equipped with thermocouples in order to follow the evolution of the temperatures in different locations (see Figure 2). Only the ordinary concrete will be studied here. Table 1 gives the composition of the ordinary concrete [5].

### Thermal Simulations Of The Wall

Because of the length of the wall, we can assume that the problem is a planar one. Only half of the wall has been meshed for the finite elements calculations due to the symmetry of the problem (see Figure 2). We assume a constant exchange coefficient  $h$  at the surface of concrete. On the symmetry axis, the heat flux is equal to zero. The initial temperature in the wall is taken equal to 20°C, as it is taken equal to 7°C in the slab. Since the slab has been previously cast, it is assumed that only thermal diffusion occurs. Therefore, only the wall hydrates and releases heat (due to hydration).

Table 1: Mix designs [5].

Aggregates [kg.m <sup>-3</sup> ]		Sand [kg.m <sup>-3</sup> ]	Cement CEM II/A 52.5 [kg.m <sup>-3</sup> ]	water-reducing plasticizer[L.m <sup>-3</sup> ]	Water [L.m <sup>-3</sup> ]
12.5/25	5/12.5				
783	316	772	350	1.04	195

It should be noted that in order to calibrate correctly the chemical affinity (Eq. 1) and the latent heat of hydration (Eq. 2), evolution of temperature in a quasi-adiabatic test must be recorded [1]. However, no such experimental data were available for the studied concretes. Therefore, we use an experimental semi-adiabatic curve obtained on a similar concrete mix, which have been modified in order to retrieve correct evolution of recorded temperature in the wall.

Figure 3 shows the evolutions of experimental and simulated temperatures at different locations (see Fig. 2). Material parameters are given in Table 2. It should be emphasized that the thermal conductivity is very important since the wall is highly reinforced (which is the case for the containment of nuclear power plants).

The numerical simulation gives reasonable results for the maximum temperatures reached in the wall.

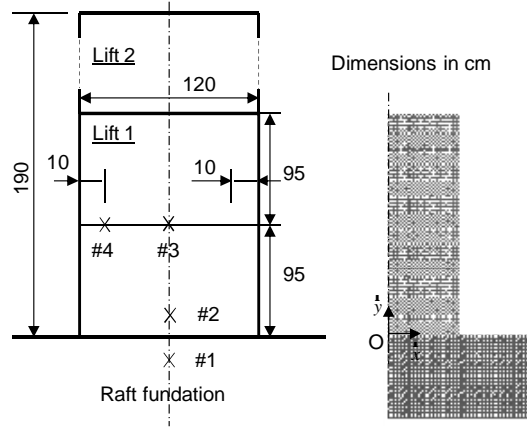


Figure 2: Geometry of the wall – locations of the thermocouples (#1, #2, #3, #4) & finite element mesh.

Table 2: Thermal parameters.

	$h$ [W.m <sup>-2</sup> .°C <sup>-1</sup> ]	$k$ [W.m <sup>-1</sup> .°C <sup>-1</sup> ]	$C$ [J.m <sup>-3</sup> .°C <sup>-1</sup> ]	$L$ [W.m <sup>-3</sup> ]	$E_a/R$ [°K <sup>-1</sup> ]
OC	3	3.05	$2.4 \times 10^6$	$154.7 \times 10^6$	4400

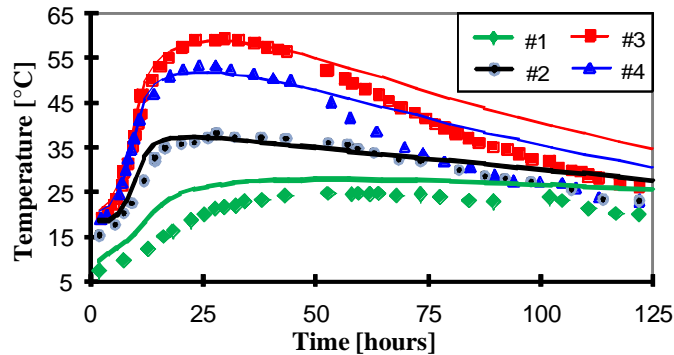


Figure 3: Comparison between experimental and simulated evolutions of temperature in the wall for the OC at different locations (see Fig. 2).

**Basic Creep Calculations**

The experimental characterisation of basic creep strain has not been performed at early-age. Therefore, we used experimental results of Laplante and Boulay [11], obtained on a concrete with a similar mix. Tests were performed on  $\Phi$  300 × 1200-mm cylindrical columns. After the form removal, the specimens were covered with self-adhesive aluminium sheets to prevent from exchanging moisture with the surrounding medium. Thus, only elastic strain, basic creep, autogeneous and thermal shrinkage are concerned. The specimens were loaded at an age of 20 hours and submitted to a given stress history (with partial and complete unloading). Temperature and strain evolutions (at the core of the

specimen) were recorded. Adiabatic tests were also performed which allows for identifying the evolutions of hydration (normalized chemical affinity, see Eq. 1) and associated release of heat.

Basic creep parameters have been identified on experimental evolutions. The corresponding identified material parameters of basic creep are given in Table 3. The comparison between experimental and numerical simulations is given in Figure 4 for the OC. No information is available concerning creep before 20 hours.

Table 3: Basic creep parameters.

	$k_{bc}^1$ [GPa]	$t_{bc}^1$ [days]	$k_{bc}^2$ [GPa]	$t_{bc}^2$ [days]	$k_{bc}^3$ [GPa]	$t_{bc}^3$ [days]
OC	$10^3$	0.1	500	1	100	10

Figure 4 underlines the fact that basic creep strains are significant at early-age and should be taken into account. The adopted model gives good agreement when the specimen is loaded. Therefore, it seems reasonable to assume that the retardation times are constant at early-age. Similar results have been obtained with others uniaxial creep models [12].

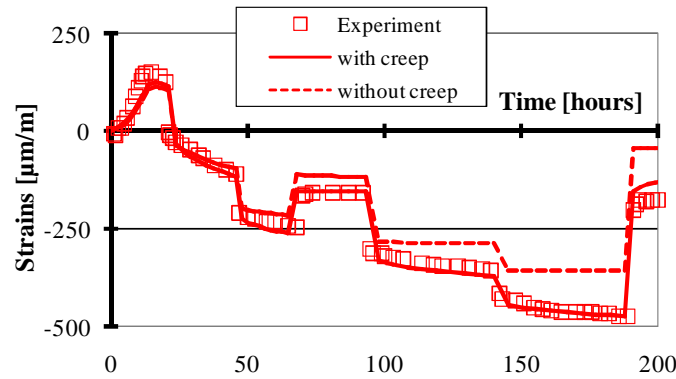


Figure 4: Comparison between experimental and simulated (without and with creep) evolutions of strains.

It should be noted that uniaxial compressive tests have been used to identify basic creep parameters. However, at early age, it is more important to predict accurately tensile creep strain, since cracking is more likely to occur in tension. Results in literature show that compressive and tensile creep strains are almost equal at early-age [13]. In our model, predicted creep strains are the same in compression and tension.

#### Mechanical Simulations Of The Wall

We assume a perfect link between concrete and the base of the wall. The strain field is assumed to be planar, since the wall is long. The mechanical parameters are given in Table 4.

In order to show the importance of creep strains at early-age, numerical simulations are performed with and without taking into account basic creep strains. Since the strains are assumed to be planar, strains perpendicular to the plan  $e_{zz}$  (Figure 2) are restrained. The evolutions of corresponding stresses  $s_{zz}$  at the middle of the structure (point number 3 in Figure 2) are plotted in Figure 5.

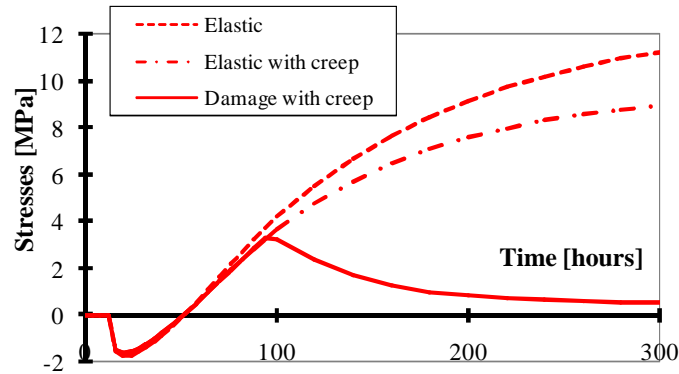
We observe that:

- At the beginning, compressive stresses rise, due to the restrain of thermal dilatation. After the temperature decreases in the core, tensile stresses occur at 40 hours, for the OC. Therefore, basic creep strain in tension must be known precisely from that moment for such a massive structure;
- Tensile stresses occur sooner (about 10 hours) when creep is taken into account. This is a negative effect of creep, but at this time, tensile strength has reached almost its final value;
- Creep strains relax slightly stresses before about 300 hours. Relaxation becomes important after about 300 hours: a decrease of stresses is observed when creep is taken into account, as a slight increase of stresses is still observed when creep is not taken into account. However, at this time, stresses overcome the tensile strength (after 110 hours for the OC);
- The computations predict cracking, even if creep is taken into account. However, on the site, 7 major crossing cracks have been recorded for the OC [5].

The last remark suggests performing rather a 3D calculus, in order to evaluate more accurately the occurrence of cracking. Indeed, for the OC, since the tensile strength is exceeding by a larger amount, more cracks should be predicted.

Table 4: Mechanical parameters

	$a$	$b$	$E_{\infty}$ [GPa]	$f_{\infty}$ [MPa]
OC	$1.2 \times 10^{-5}$	$3.10^{-5}$	32	2.5

Figure 5: Evolution of stresses  $s_{zz}$  at the middle of the structure (point #1, see Fig. 2) with respect to time

### Conclusions

A basic creep model has been modified to take into account the effect of hydration at early-age. Evolution of temperature and hydration is also predicted by using the concept of chemical affinity. Numerical simulations have been performed on a wall.

The main results obtained from this study can be summarized as follows:

- The retardation times associated to basic creep can be kept constant as suggested by de Schutter [2];
- Basic creep strains in tension should be taken into account as soon as temperature decreases (after a few days) for massive structure. However, a slight difference is observed before about ten days when creep is taken into account;
- By performing a 2D elastic analysis, cracks are predicted for OC. However, a 3D analysis should be performed in order to evaluate the number of cracks.

### References

- [1] Ulm F.-J., Coussy O., "Couplings in early-age concrete: from material modelling to structural design", *International Journal of Solids and Structures*, Vol. 35, no. 31-32, 1998, p. 4295-4311.
- [2] de Schutter G., "Degree of hydration based Kelvin model for the basic creep of early age concrete", *Materials and Structures*, Vol. 32, 1999, p. 260-265.
- [3] Mazars J., "A description of micro and macroscale damage of concrete structures", *Engineering Fracture Mechanics*, Vol 25, N°5:6, 1986.
- [4] Mazars J., Bournazel J.P., "Modelling of damage processes due to volumic variations for maturing and matured concrete", *Concrete: from material to Structure*, Arles, 1996.
- [5] Ithurrealde G., "La perméabilité vue par le maître d'ouvrage", Colloque Béton à hautes performances, Ecole Normale Supérieure, Cachan, 1989 (in french).
- [6] de Schutter G, Taerwe L (1996), Degree of hydration based description of mechanical properties of early-age concrete, *Materials and Structure*, 29, pp335-344.
- [7] Pijaudier-Cabot, G. & Bazant, Z.P. (1987), Nonlocal damage theory, *J. of Engrg. Mech. ASCE* 113: 1512-1533.
- [8] Rots, J.G. (1988), Computational modeling of concrete fracture. PhD Dissertation, Netherlands: Delft University of Technology.
- [9] Cervera, M. & Chiumenti, M. 2006. Mesh objective tensile cracking via a local continuum damage model and a crack tracking technique. *Computat. Methods Appl. Mech. Engrg.* 196: 304-320.
- [10] Hauggaard A. B., Damkilde L., Hansen, P. F. (1999), Transitional thermal creep of early age concrete *Journal of Engineering Mechanics*, 125 (4), p. 468-465.
- [11] Laplante P., Boulay C., "Evolution du coefficient de dilatation thermique du béton en fonction de sa maturité", *Materials and Structures*, Vol. 27, 1994, p. 596-605.
- [12] Guenot I., Torrenti J.M., Laplante P., "Stresses in early age concrete: comparison of different creep models", *ACI Materials Journal*, Vol. 93, no. 3, 1996, p. 254-259.
- [13] Ostergaard L., Lange D.A., Altoubat S.A., Stang H., "Tensile basic creep of early-age concrete under constant load", *Cement and Concrete Research*, 31, 2001, p. 1895-1899.